JOINT HDR AND SUPER-RESOLUTION IMAGING IN MOTION BLUR

Subeesh Vasu*, Abhijeet Shenoi†, and A. N. Rajagopalan*

*Department of Electrical Engineering, Indian Institute of Technology Madras.
†Stanford University

This is a draft version of the paper that got accepted in International Conference on Image Processing (ICIP) OCTOBER 2018. The final copyrighted version is available at
https://ieeexplore.ieee.org/abstract/document/8451735/

JOINT HDR AND SUPER-RESOLUTION IMAGING IN MOTION BLUR

Subeesh Vasu[*], *Abhijeet Shenoi*[†], *and A. N. Rajagopalan*[*]

[*]Indian Institute of Technology Madras [†]Stanford University

ABSTRACT

Images captured from consumer cameras are often prone to camera shake resulting in motion blur. Effect of motion blur is more common in high dynamic range imaging applications where multiple images are captured over a wide range of exposure settings. In this paper, we propose a unified approach to perform high dynamic range super-resolution (HDR-SR) imaging from a sequence of low dynamic range and low-resolution motion-blurred images. While existing works on HDR-SR assume the availability of blur-free input images, we propose an approach which is designed to handle blurring effects caused by the camera motion. Our approach attempts to harness the complementarity present in terms of the sensor exposure and blur to yield a high-quality image which has both higher spatial resolution as well as dynamic range. Experiments on synthetic and real examples demonstrate that the proposed method delivers state-of-the-art results.

***Index Terms*—** High dynamic range, motion blur, image restoration, super-resolution

1. INTRODUCTION

Capturing high-quality image is an important goal of modern photography. Dynamic range and spatial resolution are the most desirable properties determining the quality of digital images. However, there exist multiple hurdles to achieve higher dynamic range and resolution in captured images. First of all, digital camera sensors are designed to capture only a limited range of the scene irradiance. This limitation results in over-/under-exposed regions in an image captured with a fixed exposure duration. HDR imaging technique [1, 2] was developed to overcome this limitation, wherein the attempt was to recover entire scene irradiance by algorithmically integrating the information contained in multiple low dynamic range (LDR) images captured at different exposure settings. On the other hand, image super-resolution (SR) algorithms were developed to overcome the resolution limitations suffered by the digital cameras. Multiple images captured using different camera poses have differences in their sampling grids. This possibility is explored by multi-image SR methods to obtain a high-resolution (HR) image from multiple low-resolution (LR) images captured using a moving camera [3, 4]. A common property shared by HDR and SR imaging is the use of multiple input images which often carries cues that can extend the intensity range as well as the spatial resolution. This is the key motivation behind recent attempts [5–10] to perform joint HDR-SR imaging, by combining both the motion and intensity information available in the input images.

Despite the high popularity, existing HDR and SR methods work under strong assumptions on image capturing conditions, which often limits their practical applicability. Majority of the literature in HDR imaging [1,2,11] as well as multi-image SR [12–14] was developed assuming the availability of blur-free input images and hence works exceedingly well when the images are acquired using a tripod. With the introduction of light-weight, hand-held, photographic devices, images are now increasingly susceptible to camera shake due to unsteady hands, resulting in significant amount of motion blur. While there were few attempts to individually perform HDR [15, 16] and SR [17–19] from motion blurred images, all existing methods which perform a joint high dynamic range super-resolution (HDR-SR) imaging works under the strong assumption of blur-free input images. The potential to obtain a super-resolved HDR image while accounting for the blur effects in input images remains unexplored.

In this paper, we propose a unified approach to perform HDR-SR imaging from multiple motion-blurred input images. Our proposed approach is designed to handle both uniform and non-uniform blur effects [20] induced by camera motion. Since the input images themselves are blurry, we also need to estimate the camera motion causing the blur. It is well-known that saturation regions violate the linearity in image formation [21]. Since we work with different exposure input images, it is thus important to carefully model the image formation mechanism to ensure the robustness of the estimation process in handling such non-linearities. Our proposed approach relies on an alternating minimization scheme wherein we simultaneously solve for the HR camera motion as well as a blur-free HDR-SR image while accounting for the saturation effects in input images.

The main contributions of our work are listed below:

- This is the first attempt to formally address the problem of estimating the latent HDR-HR image given a set of LDR-LR observations that are captured at different exposures and are blurred due to incidental camera shake.
- We introduce an HDR-SR image formation model to explain the relation between blur-free HDR-HR image and blurry LDR-LR images. We then propose an elegant alternating minimization scheme which solves for the underlying HR camera motion as well as the HDR-HR latent image while accounting for the damaging influences of the saturation regions in input images.

2. IMAGE FORMATION MODEL

Let $\mathbf{g} \in \mathbb{R}^{mn\times 1}$ be the image captured by the camera at the irradiance domain and $\mathbf{f} \in \mathbb{R}^{mn\times 1}$ be the latent scene irradiance. We use the column vector representation of images, for example, $\mathbf{g}$ is a column vector formed by lexicographically arranging the elements of the 2D image $g \in \mathbb{R}^{m\times n}$. In conventional cameras, during image capture, the irradiance of the scene $\mathbf{f}$ get aggregated in the camera sensors for a duration called exposure period (η_e). If there exists no relative motion between the scene and camera, all the sensors will get exposed to the same scene point and the captured image will be blur-free. When the camera undergoes motion, irradiances from different scene points will get accumulated in each sensor resulting in a motion blurred image. Using the projective homography model,

the motion blurred image $\mathbf{g}$ can be expressed as an average of the warped instances of $\mathbf{f}$ as [22, 23]

$$\mathbf{g} = \int_0^{\eta_e} \mathbf{H}_\tau(\mathbf{f}) d\tau \tag{1}$$

where $\mathbf{H}_\tau(\mathbf{f})$ refers to the warped irradiance obtained by applying the homography $\mathbf{H}_\tau$ corresponding to the time instant τ. The homography $\mathbf{H}_\tau$ ([22]) is used to relate the pixel positions in the latent irradiance image $\mathbf{f}$ to that of its projection onto the camera sensor at time τ. $\mathbf{H}_\tau$ can be expressed as a function of camera intrinsic parameters and camera pose vector p_τ as follows.

$$\mathbf{H}_\tau = \mathbf{K}\left(\mathbf{R}_\tau + \mathbf{t}_\tau \frac{[0\ 0\ 1]}{d}\right)\mathbf{K}^{-1} \tag{2}$$

where $\mathbf{R}_\tau$, and $\mathbf{t}_\tau$ are the rotation and translational matrices corresponding to the camera pose p_τ, and d is the distance of the scene point from camera. $\mathbf{K}$ is the camera intrinsic matrix, which is a function of the focal length of the camera.

Next we will account for resolution effects in image capture. We assume that the HR image $\mathbf{g}$ of a real world scene should have been captured by a sensor array of larger resolution $M \times N$, whereas since the camera sensor array resolution was only $M' \times N'$, the captured image $\mathbf{l}$ has a resolution which is s (where $s = M'/M = N'/N$) times lower as compared to $\mathbf{g}$. Following conventional SR methods [17], we model the relation between $\mathbf{g}$ and $\mathbf{l}$ through a decimation matrix $\mathbf{D}$ as

$$\mathbf{l} = \mathbf{D}\mathbf{g} = \mathbf{D}\int_0^{\eta_e} \mathbf{H}_\tau(\mathbf{f}) d\tau \tag{3}$$

where the decimation operator $\mathbf{D} \in \mathbb{R}^{M'N' \times MN}$ is designed to mimic the behaviour of the digital sensors. The decimation process consists of a convolution with the sensor point spread function (PSF), followed by sampling. We use a Gaussian function to model the sensor PSF since it is best suited to mimic the real camera sensor [24]. The sampling operation is done as the multiplication of image by a sum of delta functions placed on an evenly spaced grid. Here $\mathbf{D}$ encode the effects of both the sensor PSF and sampling altogether.

Limited storage capacity of the sensors causes saturated regions in the captured image. If the integrated irradiance is below a threshold, or above a certain value, it will result in under- or over-exposed regions. We can model this effect by introducing a saturation clipping function c as

$$\mathbf{l}_c = c\left(\mathbf{D}\int_0^{\eta_e} \mathbf{H}_\tau(\mathbf{f}) d\tau\right) \tag{4}$$

where c is given by

$$c(x) = \begin{cases} 0 & x < LowerBound \\ 1 & x > UpperBound \\ x & otherwise \end{cases} \tag{5}$$

Here we consider images with values ranging from 0 to 1, c assign the values 0 or 1 if the signal captured by the sensors goes below or above the allowed limits.

In cameras, the image obtained from the output of the sensors undergoes different kinds of transformation before getting converted into final pixel values. The non-linear mapping from irradiance to pixel values can be modeled using a camera response function (CRF). The CRF (ρ) can be used to relate the final image and the output from camera sensors as

$$\mathbf{k} = \rho\left(c\left(\mathbf{D}\int_0^{\eta_e} \mathbf{H}_\tau(\mathbf{f}) d\tau\right)\right) \tag{6}$$

In our work, we first invert the effect of CRF and works with the images in irradiance domain to perform HDR-SR. Hence, for the remainder of this paper, we will ignore the effect of CRF from consideration.

2.1. Discrete modeling via Motion Density Function

Despite the camera trajectory being continuous, for the sake of tractability, we use the discrete equivalent model of the camera motion [16, 22]. To device the discrete model, consider a discrete camera pose space Γ comprising of a collection of finite number of camera poses. Camera motion in Γ can be represented in terms of a motion density function (MDF) [16, 22] which maps every camera pose p in Γ to a non-negative real number i.e., $\mathbf{w}(p) : p(\in \Gamma) \rightarrow \mathbb{R}^+$. The value of $\mathbf{w}(p)$ denotes the fraction of the total exposure duration for which the camera stayed at p, and therefore $\sum_{p\in\Gamma} \mathbf{w}(p) = \eta_e$. Now we can re-write the integral in Eq. 3 by a summation in terms of MDF as

$$\mathbf{l} = \mathbf{D}\sum_{p\in\Gamma} \mathbf{w}(p)\mathbf{H}_p(\mathbf{f}) \tag{7}$$

Discrete formulation allows to express the relation between the blurred LR images and clean HR image in the form of linear equations. Eq. 3 can now be expressed in two different forms of matrix-vector multiplication as [23]

$$\mathbf{l} = \mathbf{D}\mathbf{F}\mathbf{w} = \mathbf{D}\mathbf{W}\mathbf{f} \tag{8}$$

where $\mathbf{F} \in \mathbb{R}^{MN \times |P|}$ ($|P| \rightarrow$ total number of poses in P) is a matrix formed of the HR irradiance map $\mathbf{f}$, with i^{th} column of $\mathbf{F}$ being the warped form of $\mathbf{f}$, warped according to corresponding camera pose $p \in \Gamma$. $\mathbf{W} \in \mathbb{R}^{MN \times MN}$ is a large sparse matrix, containing non-zero values derived from MDF $\mathbf{w}$ and homographies of corresponding poses. Intuitively, rows of $\mathbf{W}$ reprsents local blur filters which can operate on pixels of $\mathbf{f}$ to yield the blurred image $\mathbf{g}$.

2.2. Multi-exposure images

To capture the entire irradiance of the scene one need to capture multiple images with different exposure settings. We can now relate the i^{th} LR image $\mathbf{l}_c^i$ captured with exposure time η_e^i to the HR scene irradiance $\mathbf{f}$ as

$$\mathbf{l}_c^i = c\left(\mathbf{D}\sum_{p\in\Gamma} \mathbf{w}^i(p)\mathbf{H}_p(\mathbf{f})\right), \ \text{for} \ i = 1, .., \vartheta \tag{9}$$

where $\mathbf{w}^i$ ($\sum_{p\in\Gamma} \mathbf{w}^i(p) = \eta_e^i$) is the MDF representing HR motion of the camera involved in the image formation of $\mathbf{l}_c^i$ and ϑ is the total number of LR images which we capture. Next we will discuss our proposed approach for the recovery of HR irradiance map $\mathbf{f}$ from a set of LDR-LR images $\mathbf{l}_c^i (i = 1, .., \vartheta)$.

3. RECOVERING HR IRRADIANCE MAP

Given a set of LDR-LR images $\mathbf{l}_c^i (i = 1, .., \vartheta)$, estimation of $\mathbf{f}$ is a non-trivial task. This is because both $\mathbf{w}^i$ and $\mathbf{f}$ is unknown, and one

need to solve for both the unknowns simoultaneously. To resolve this ambuiguity, we enforce priors on **f** and **w**, and iteratively refine the estimates of **f** and **w** until convergence.

3.1. HR image estimation

To solve for **f** from known estimate of camera motion, we solve the following form of optimization problem

$$\arg\min_{\mathbf{f}} \sum_{i=1}^{\vartheta} \left|\left| \boldsymbol{\chi}^i \left(\mathbf{l}_c^i - \mathbf{D} \sum_{p \in \Gamma} \mathbf{w}^i(p) \mathbf{H}_p(\mathbf{f}) \right) \right|\right|_2^2 + \lambda_{\mathbf{f}} ||\nabla \mathbf{f}||_1 \tag{10}$$

where ∇ refers to the gradient operator. In Eq. 10, the first term is the data cost which ensure that the estimated image is consistent with the input LR images. The second term enforces L_1 norm sparsity prior on image gradients ($\nabla \mathbf{f}$), by which we can ensure an outlier robust restoration of image [25]. $\boldsymbol{\chi}^i$ represents a saturation mask matrix associated with $\mathbf{l}_c^i$. $\boldsymbol{\chi}^i$ have The diagonal entries of $\boldsymbol{\chi}^i$ is formed by applying a Tukey window [16] on $\mathbf{l}_c^i$. Tukey window assigns low weights to the pixels in $\mathbf{l}_c^i$ which are close to saturation. Since the weight for the errors induced by saturated pixels is low, use of $\boldsymbol{\chi}^i$ alleviates the negative influences in the datacost caused by the saturated pixels in $\mathbf{l}_c^i$. Using Eq. 8, Eq. 10 can be simplified to regularized least square formulation of the form

$$\arg\min_{\mathbf{f}} \sum_{i=1}^{\vartheta} ||\boldsymbol{\chi}^i \mathbf{l}_c^i - \chi^i \mathbf{D} \mathbf{W}^i \mathbf{f}||_2^2 + \lambda_{\mathbf{f}} ||\nabla \mathbf{f}||_1 \tag{11}$$

where $\mathbf{W}^i$ is derived from the known MDF vector $\mathbf{w}^i$.

3.2. Camera motion estimation

Existing works on motion deblurring [25, 26] have shown that use of salient edges in the image for motion estimation can deliver accurate results while facilitating faster convergence. Following this observation, we apply bilateral filtering followed by shock filtering on the estimated latent image to yield the desired salient edges. More details of this edge prediction scheme can be found in [26]. The bilateral filter is primarily used to suppress noise and small edges whereas the shock filter is used to restore the strong edges. To obtain an estimate of HR camera motion $\mathbf{w}^i$ corresponding to i^{th} LR image $\mathbf{l}_c^i$, we solve the following optimization problem.

$$\arg\min_{\mathbf{w}^i} \left|\left| \boldsymbol{\chi}^i \left(\nabla \mathbf{l}_c^i - \mathbf{D} \sum_{p \in \Gamma} \mathbf{w}^i(p) \mathbf{H}_p(\tilde{\nabla \mathbf{f}}) \right) \right|\right|_2^2 + \lambda_{\mathbf{w}}^i ||\mathbf{w}^i||_1 \tag{12}$$

where we use only the gradients of the images to compute the camera motion, $\tilde{\nabla \mathbf{f}}$ refers to the salient edges of **f** obtain through our edge prediction step. We use an L_1 norm prior on **w**, to enforce the natural sparsity of camera motion trajectory (since camera motion will occupy only a few poses in the entire pose space). Eq. 12 can be simplified to

$$\arg\min_{\mathbf{w}^i} ||\boldsymbol{\chi}^i \nabla \mathbf{l}_c^i - \chi^i \mathbf{D} \tilde{\mathbf{F}} \mathbf{w}^i||_2^2 + \lambda_{\mathbf{w}}^i ||\mathbf{w}^i||_1 \tag{13}$$

where $\tilde{\mathbf{F}}$ is formed from $\tilde{\nabla \mathbf{f}}$.

Algorithm 1 HDR-SR Image Recovery from a Set of Non-Uniformly Motion Blurred LR LDR Images.

Input: Set of LR LDR images $\{\mathbf{k}^i\}_{i=1}^{\vartheta}$ captured using multi-expsoure settings.
Output: HR HDR irradiance map **f**.

1: Obtain the LR LDR images in irradiance domain $\{\mathbf{l}_c^i\}_{i=1}^{\vartheta}$ by inverse mapping with CRF
2: **for** $scale = \mu_1 : \mu_r$ **do**
3: **if** $scale = \mu_1$, **do**
4: Downsample $\mathbf{l}_c^1$ by a factor of $\frac{\mu_1}{2}$ to obtain initial estimate of $\widehat{\mathbf{f}}$
5: Solve Eq. 13 to obtain initial estimate of $\{\widehat{\mathbf{w}}^i\}_{i=1}^{\vartheta}$
6: **else do**
7: Initialize MDF with the bilinear interpolated form of $\{\widehat{\mathbf{w}}^i\}_{i=1}^{\vartheta}$ from previous scale
8: **end if**
9: **for** iteration $\xi = 1 : \xi_{max}$ **do**
10: Obtain HR image estimate $\widehat{\mathbf{f}}$ by solving Eq. 11
11: Estimate MDF, $\{\widehat{\mathbf{w}}^i\}_{i=1}^{\vartheta}$ by solving Eq. 13
12: **end for**
13: **end for**
14: Obtain final HR HDR image $\widehat{\mathbf{f}}$ by solving Eq. 11.

3.3. Implementation details

Since both **f** and $\mathbf{w}_i$ are unknowns, to yield the desired solution we employ an AM scheme wherein we refine the estimates of both **f** and $\mathbf{w}_i$ until convergence. An overview of our proposed AM scheme is provided in Algorithm 1. Akin to existing methods [23, 25, 26], to ensure convergence for the case of large motion blur, we perform the AM in a scale space fashion. To estimate the camera motion at lower scales, we use the downsampled versions of the captured LR images. At the lowest scale, we use LR LDR images obtained with a downsampling factor of μ_1 to estimate the camera motion. We downsample the lowest exposure image by a factor of $\frac{\mu_1}{2}$ to yield the initial estimate of HR HDR image at that scale. Salient edges predicted from this initial estimate **f** is then used to recover HR camera motions corresponding to all LDR images using Eq. 13. The estimate of HR camera motion is then refined by alternatively minimizing the problems Eq. 11 and Eq. 13 until convergence. The estimation unit in each scale is initialized with the up-sampled version of MDF estimates from the previous scale. Note that, the main objective of the alternating minimization is to obtain an accurate estimate of the underlying camera motion. To obtain the final HR irradiance map, we solve Eq. 11 using the MDF estimate obtained from the AM unit.

In our implementation, the pose space used for MDF estimation is modified at every iteration to limit its size. This is done by randomly sampling in and around the most dominant poses at every iteration, by using a Gaussian distribution as the sampling distribution [27]. This kind of a pose-space reduction scheme has multiple advantages. First of all, we can better regularize the MDF estimation problem, since we are effectively reducing the dimension of unknowns in the subsequent iterations. Moreover, since the size of $\tilde{\mathbf{F}}$ depends on the number of poses in the search space, the dimensionality reduction can significantly reduce the computational time and memory requirements for the optimization in Eq. 13.

For our real experiments, we employ the approach in [2] to obtain the CRF through camera calibration. As the first step, we will convert each LR image into the irradiance domain by applying an inverse mapping based on the estimated CRF. These LDR-LR images

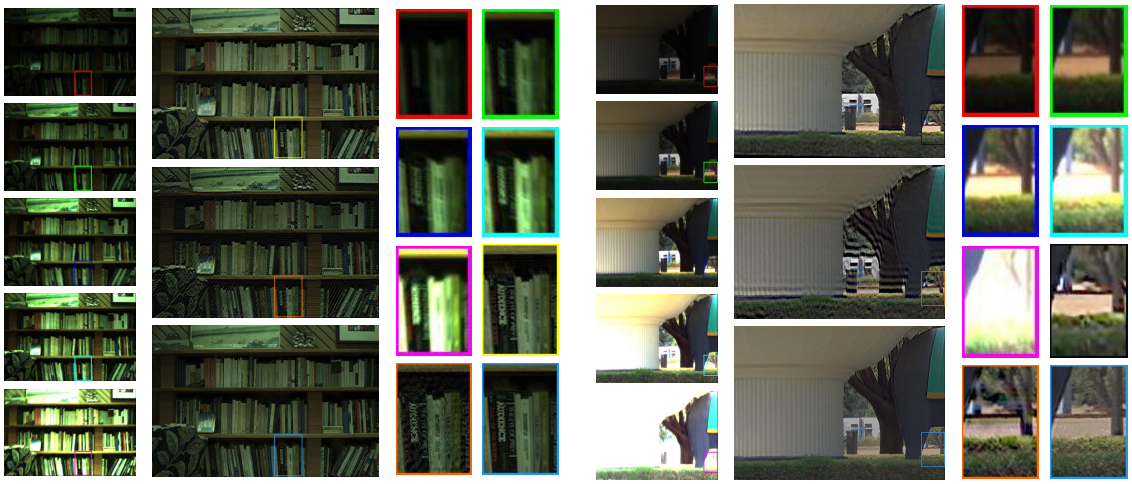

Fig. 1. HDR-SR imaging: Synthetic and real examples (left and right). Columns 1,5: Input LDR images with varying exposure values. Tone mapped HR HDR image recovered using [16] $\rightarrow$ [31] (1^{st} row, column 2), [31] $\rightarrow$ [16]) (2^{nd} row, columns 2,6), [32] $\rightarrow$ [33] $\rightarrow$ [31] (1^{st} row, column 6), and proposed approach (3^{rd} row, columns 2,6). Columns 3-4, 7-8: Zoomed-in patches from images in columns 1-2, 5-6.

are then used within an alternating minimization (AM) scheme to yield the desired HR HDR irradiance image which is then remapped to the low dynamic range of the display by tone mapping [28]. All our experiments are done for a super-resolution factor (s) of 2. To solve Eq. 11 and 13 we employ alternating direction method of multipliers (ADMM) algorithm [29,30]. The values of $\lambda_{\mathbf{f}}$, $\lambda^i_{\mathbf{w}}$, and ξ_{max} was set (empirically found) to 0.003 0.01, and 5 respectively. For scale-space implementation, we set the total number of scales (r) to 5 with $\mu_1 = 2\sqrt{2}$, and $\mu_{i+1} = \dfrac{\mu_i}{\sqrt{2}}$.

4. EXPERIMENTS

In this section, we demonstrate the effectiveness of our proposed approach on synthetic as well as real images. Since there exist no other methods which handle the problem of HDR-SR from motion blurred images, we compare our results with three possible combination of most recent works on motion deblurring, HDR and SR. First approach is to apply single image SR algorithm of [31] on the LR HDR image obtained from [16] (we name this approach as ([16] $\rightarrow$ [31]). Second approach is to apply single image SR algorithm of [31] on all input images and then obtain HDR-HR image using [16] ([31] $\rightarrow$ [16]). Third approach is to individually deblur each LR LDR employing [32] and use the resulting images to obtain a single LR HDR image using the outlier-robust HDR method in [33], and then apply [31] to recover the HR HDR image ([32] $\rightarrow$ [33] $\rightarrow$ [31]).

In [16], MDF is derived from PSF estimates obtained through deblurring of local patches. Since local PSF estimates are often prone to errors, the effectiveness of this approach in capturing the camera motion is limited. For the case of [16] $\rightarrow$ [31], the ability to resolve details is marginal since the SR unit relies only on a single image. At the same time, the artifacts generated by [16] gets amplified while attempting to super-resolve using [31]. On the other hand, super-resolution of LR blurry images can result in inconsistencies between the pixel intensities and the underlying camera motion which caused the blur. The presence of such deviations from the blur model will induce artifacts in the restoration results from [31] $\rightarrow$ [16]. The approach [32] $\rightarrow$ [33] $\rightarrow$ [31] suffer from the cumulative effects of deblurring artifacts, pixel inconsistencies across images (caused by deblurring artifacts), and lack of details due to reliability on single image for SR. In contrary to all these approaches, since our model exploits the direct relation between MDF and the entire image, it is expected to deliver an accurate estimate of camera motion. Also, unlike [16], we solve for the HR camera motion. Our joint optimization scheme attempt to recover both HR camera motion and HR irradiance by exploiting the direct relation between the desired estimates and inputs, therefore guaranteeing significant performance improvement.

For synthetic experiments, we generate LDR-LR motion blurred images using Eq. 4. We use HDR image from [34] as the ground truth (GT) irradiance ($\mathbf{f}$) and camera trajectories from [20] to simulate the effect of camera motion. First four columns of Fig. 1 shows a synthetic example wherein we have used 5 LDR-LR images (Fig. 1, column 1) generated with different exposure ratios as the inputs. The remaining columns correspond to a real example for which the input images were captured using a Canon 60D camera with different exposure settings. Note that, all the three approaches which we use for HDR-HR recovery are able to integrate the well-exposed regions from different images. However, as is evident from Fig. 1, the ineffectiveness of competing approaches (as we discussed earlier) results in lack of details and/or amplified artifacts. Whereas our unified approach correctly integrates the desired information from the inputs and delivers an artifact-free detail-rich HDR-HR image. Additional results are provided in the supplementary material.

5. CONCLUSION

In this paper, we have addressed the problem of recovering an HDR-HR image from a sequence of non-uniformly motion blurred LDR-LR images captured at multiple exposure settings. To recover an accurate estimate of camera motion, our proposed approach alternatively minimizes the problem of camera motion estimation and image estimation while simultaneously accounting for the negative influences caused by the saturation regions in the input images. Our synthetic and real experiments have shown the efficacy of the proposed algorithm in advancing the state-of-the-art. As future work, we plan to extend our approach to handle challenging cases of dynamic objects and 3D scenes.

6. REFERENCES

[1] S. Mann and R. W. Picard, "On being 'undigital' with digital cameras: Extending dynamic range by combining differently exposed pictures," in *Proceedings of IS & T*, 1995, pp. 442–448.

[2] P. E. Debevec and J. Malik, "Recovering high dynamic range radiance maps from photographs," in *Proc. ACM SIGGRAPH*, 1997.

[3] S. C. Park, M. K. Park, and M. G. Kang, "Super-resolution image reconstruction: a technical overview," *IEEE SPM*, vol. 20, no. 3, pp. 21–36, 2003.

[4] S. Farsiu, D. Robinson, M. Elad, and P. Milanfar, "Advances and challenges in super-resolution," *International Journal of Imaging Systems and Technology*, vol. 14, no. 2, pp. 47–57, 2004.

[5] B. K. Gunturk and M. Gevrekci, "High-resolution image reconstruction from multiple differently exposed images," *SPL*, vol. 13, no. 4, pp. 197–200, 2006.

[6] A. A. Rad, L. Meylan, P. Vandewalle, and S. Süsstrunk, "Multidimensional image enhancement from a set of unregistered and differently exposed images," in *Electronic Imaging*. International Society for Optics and Photonics, 2007, pp. 649808–649808.

[7] F. Schubert, K. Schertler, and K. Mikolajczyk, "A hands-on approach to high-dynamic-range and superresolution fusion," in *Applications of Computer Vision (WACV), Workshop on*. IEEE, 2009, pp. 1–8.

[8] H. Zimmer, A. Bruhn, and J. Weickert, "Freehand hdr imaging of moving scenes with simultaneous resolution enhancement," in *Computer Graphics Forum*. Wiley Online Library, 2011, vol. 30, pp. 405–414.

[9] T. Bengtsson, I. Y. H. Gu, M. Viberg, and K. Lindström, "Regularized optimization for joint super-resolution and high dynamic range image reconstruction in a perceptually uniform domain," in *ICASSP*, 2012, pp. 1097–1100.

[10] Y. Traonmilin and C. Aguerrebere, "Simultaneous high dynamic range and superresolution imaging without regularization," *SIAM Journal on Imaging Sciences*, vol. 7, no. 3, pp. 1624–1644, 2014.

[11] Greg Ward, "Fast, robust image registration for compositing high dynamic range photographs from hand-held exposures," *Journal of graphics tools*, vol. 8, no. 2, pp. 17–30, 2003.

[12] R. C. Hardie, K. J. Barnard, and E. E. Armstrong, "Joint map registration and high-resolution image estimation using a sequence of undersampled images," *TIP*, vol. 6, no. 12, pp. 1621–1633, 1997.

[13] C. A. Segall, A. K. Katsaggelos, R. Molina, and J. Mateos, "Bayesian resolution enhancement of compressed video," *TIP*, vol. 13, no. 7, pp. 898–911, 2004.

[14] N. A. Woods, N. P. Galatsanos, and A. K. Katsaggelos, "Stochastic methods for joint registration, restoration, and interpolation of multiple undersampled images," *TIP*, vol. 15, no. 1, pp. 201–213, 2006.

[15] P. Y. Lu, T. H. Huang, M. S. Wu, Y. T. Cheng, and Y. Y. Chuang, "High dynamic range image reconstruction from hand-held cameras," in *CVPR*, 2009, pp. 509–516.

[16] C. S. Vijay, C. Paramanand, A. N. Rajagopalan, and R. Chellappa, "Non-uniform deblurring in hdr image reconstruction," *TIP*, vol. 22, no. 10, pp. 3739–3750, 2013.

[17] F. Sroubek, G. Cristóbal, and J. Flusser, "A unified approach to superresolution and multichannel blind deconvolution," *TIP*, vol. 16, no. 9, pp. 2322–2332, 2007.

[18] H. Zhang and L. Carin, "Multi-shot imaging: joint alignment, deblurring and resolution-enhancement," in *CVPR*, 2014, pp. 2925–2932.

[19] Ziyang Ma, Renjie Liao, Xin Tao, Li Xu, Jiaya Jia, and Enhua Wu, "Handling motion blur in multi-frame super-resolution," in *CVPR*, 2015, pp. 5224–5232.

[20] R. Köhler, M. Hirsch, B. Mohler, B. Schölkopf, and S. Harmeling, "Recording and playback of camera shake: Benchmarking blind deconvolution with a real-world database," in *ECCV*. Springer, 2012, pp. 27–40.

[21] O. Whyte, J. Sivic, and A. Zisserman, "Deblurring shaken and partially saturated images," *IJCV*, 2014.

[22] A. Gupta, N. Joshi, C. Z. Lawrence, M. Cohen, and B. Curless, "Single image deblurring using motion density functions," *ECCV*, pp. 171–184, 2010.

[23] O. Whyte, J. Sivic, A. Zisserman, and J. Ponce, "Non-uniform deblurring for shaken images," in *CVPR*, 2010.

[24] David Capel, "Image mosaicing," in *Image Mosaicing and Super-resolution*, pp. 47–79. Springer, 2004.

[25] L. Xu and J. Jia, "Two-phase kernel estimation for robust motion deblurring," in *ECCV*, 2010, pp. 157–170.

[26] Sunghyun Cho and Seungyong Lee, "Fast motion deblurring," in *TOG*. ACM, 2009, vol. 28, p. 145.

[27] Zhe Hu and Ming-Hsuan Yang, "Fast non-uniform deblurring using constrained camera pose subspace.," in *BMVC*, 2012, vol. 2, p. 4.

[28] Raanan Fattal, Dani Lischinski, and Michael Werman, "Gradient domain high dynamic range compression," in *TOG*. ACM, 2002, vol. 21, pp. 249–256.

[29] S. Boyd, N. Parikh, E. Chu, B. Peleato, and J. Eckstein, "Distributed optimization and statistical learning via the alternating direction method of multipliers," *Foundations and Trends® in Machine Learning*, vol. 3, no. 1, pp. 1–122, 2011.

[30] Shuochen Su and Wolfgang Heidrich, "Rolling shutter motion deblurring," in *CVPR*, 2015, pp. 1529–1537.

[31] C. Cruz, R. Mehta, V. Katkovnik, and K. O. Egiazarian, "Single image super-resolution based on wiener filter in similarity domain," *TIP*, vol. 27, pp. 1376–1389, 2018.

[32] Subeesh Vasu and AN Rajagopalan, "From local to global: Edge profiles to camera motion in blurred images," in *CVPR*, 2017, pp. 4447–4456.

[33] Tae-Hyun Oh, Joon-Young Lee, Yu-Wing Tai, and In So Kweon, "Robust high dynamic range imaging by rank minimization," *TPAMI*, vol. 37, no. 6, pp. 1219–1232, 2015.

[34] B. Funt and L. Shi, "The rehabilitation of maxrgb," in *Color and Imaging Conference*, 2010, pp. 256–259.